Glaucomatous Focal Perfusion Loss in the Macula Measured by Optical Coherence Tomographic Angiography

AIYIN CHEN, PING WEI, JIE WANG, LIANG LIU, ACNER CAMINO, YUKUN GUO, OU TAN, YALI JIA, AND DAVID HUANG

• PURPOSE: To measure low perfusion area (LPA) and focal perfusion loss (FPL) in the macula using optical coherence tomography (OCT) angiography (OCTA) for glaucoma.

• DESIGN: Prospective, cross-sectional "case-control" comparison study.

• METHODS: A total of 60 patients with primary open-angle glaucoma (POAG) and 37 healthy participants were analyzed. AngioVue 6 × 6-mm high-definition (400 × 400 transverse pixels) macular OCTA scans were performed on one eye of each participant. Flow signal was calculated using the split-spectrum amplitude-decorrelation angiography algorithm. En face ganglion cell layer plexus (GCLP) and superficial vascular complex (SVC) images were generated. Using custom software, vessel density (VD) maps were obtained by computing the fraction of area occupied by flow pixels after low-pass filtering by local averaging 41 × 41 pixels. LPA was defined by local VD below 0.5 percentile over a contiguous area above 98.5 percentile of the healthy reference population. The FPL was the percentage VD loss (relative to normal mean) integrated over the LPA.

• RESULTS: Among patients with POAG, 30 had perimetric and 30 had preperimetric glaucoma. The $LPA_{GCLP\text{-}VD}$ was 0.16±0.38 mm^2 in normal and 5.78±6.30 mm^2 in glaucoma subjects ($P < .001$). The $FPL_{GCLP\text{-}VD}$ was 0.20%±0.47% in normal and 7.52%±8.84% in glaucoma subjects ($P < .001$). The perimetric glaucoma diagnostic accuracy, measured by the area under the receiver operating curve, was 0.993 for $LPA_{GCLP\text{-}VD}$ and 0.990 for $FPL_{GCLP\text{-}VD}$. The sensitivities were, respectively, 96.7% and 93.3% at 95% specificity. The $LPA_{GCLP\text{-}VD}$ and $FPL_{GCLP\text{-}VD}$ had good repeatability (0.957 and 0.952 by intraclass correlation coefficient). Diagnostic accuracy was better than GCLP VD (AROC 0.950, sensitivity 83.3%) and OCT ganglion cell complex (GCC) thickness (AROC 0.927, sensitivity 80.0%) and GCC focal loss volume (AROC 0.957, sensitivity 80.0%). The $LPA_{GCLP\text{-}VD}$ and $FPL_{GCLP\text{-}VD}$ correlated well with central VF mean deviations (Pearson $r = –0.716$ and –0.705 respectively, both $P < .001$).

• CONCLUSION: Assessment of macular FPL using OCTA is useful in evaluating glaucomatous damage. (Am J Ophthalmol 2024;268: 181–189. © 2024 Elsevier Inc. All rights are reserved, including those for text and data mining, AI training, and similar technologies.)

Glaucoma causes irreversible damage to the retina and optic nerve, which leads to subsequent visual field (VF) and vision loss. Although it is widely accepted that glaucoma damages start at the optic nerve head, macular damages can occur in all stages of glaucoma, and it can occur in early glaucoma with either deep focal or shallow widespread pattern.[1,2] The metabolically active retinal ganglion cells are most concentrated in the macula[3] and rely heavily on a network of capillary for their oxygen and nutrient supply.[4] Measuring either neural tissue thickness or blood flow in the macula has been proposed as a way to diagnose and monitor glaucoma.[5-9]

Optical coherence tomography (OCT) angiography (OCTA) is a noninvasive imaging modality to evaluate blood flow, and reduced capillary perfusion using OCTA in glaucoma patients have been found in the optic nerve head, peripapillary nerve fiber layer plexus, and macular superficial vascular complex compared with healthy subjects.[10-15] Decreased vessel density (VD) in the macula region also has been demonstrated using OCTA in primary open angle glaucoma,[5] and this decrease can progress with time.[16] However, VD in the macula may not be homogenous,[5] and glaucoma damage in the macula can be focal or diffuse. A map highlighting either focal or diffuse abnormal perfusion could provide earlier detection and differentiation from other conditions (ie, optic neuropathy and retinal diseases).[17-19] Focal loss analysis in macular OCT was found to be particularly powerful in early glaucoma diagnosis and correlation with VF defect.[1]

Therefore, it is desirable to develop methods for abnormal perfusion analysis using OCTA. In a previous study,

AJO.com Supplemental Material available at AJO.com.

Aiyin Chen and Ping Wei are co–first authors and contributed equally to this study.

Accepted for publication July 5, 2024.

From the Casey Eye Institute and Department of Ophthalmology, Oregon Health and Science University, Portland, Oregon, USA.

Inquiries to David Huang, Casey Eye Institute, Oregon Health and Science University, Portland, Oregon, USA; e-mail: davidhuang@alum.mit.edu

0002-9394/$36.00
https://doi.org/10.1016/j.ajo.2024.07.008

we developed a novel OCTA image processing algorithm to map and quantify focal perfusion defects associated with glaucoma in the peripapillary region.[20] We now apply this novel method to the macula using a higher-resolution scan and a larger cross-sectional population of open angle glaucoma patients and healthy subjects.

METHODS

• **STUDY POPULATION:** This prospective, cross-sectional case-control comparison study was performed from May 22, 2017, to July 18, 2019, at the Casey Eye Institute, Oregon Health & Science University (OHSU). The research protocols were approved by the Institutional Review Board at OHSU and carried out in accordance with the tenets of the Declaration of Helsinki. Written informed consent was obtained from each participant.

All participants were part of the Functional and Structural Optical Coherence Tomography for Glaucoma study (R01 EY023285). The inclusion criteria for the perimetric glaucoma (PG) group were (1) an optic disc rim defect (thinning or notching) or retinal nerve fiber layer (NFL) defect visible on slitlamp biomicroscope and (2) a consistent glaucomatous pattern, on both qualifying Humphrey SITA 24-2 VFs, meeting at least 1 of the following criteria: pattern SD outside normal limits ($P < .05$) or glaucoma hemifield test outside normal limits. Eyes in the preperimetric glaucoma (PPG) group met the biomicroscopic criteria (1) but not criteria (2) as above.

For the healthy group, the inclusion criteria were as follows: (1) no evidence of retinal pathology or glaucoma, (2) a normal Humphrey 24-2 VF, (3) intraocular pressure <21 mm Hg, (4) central corneal pachymetry >500 μm, (5) no chronic ocular or systemic corticosteroid use, (6) an open angle on gonioscopy, (7) a normal-appearing optic nerve head and NFL, and (8) symmetric optic nerve heads between the left and right eye. The exclusion criteria for both groups were as follows: (1) best-corrected visual acuity less than 20/40, (2) age <40 or >80 years, (3) spherical equivalent refractive error of >+3.00 diopters (D) or <−7.00 D, (4) previous intraocular surgery except for an uncomplicated cataract extraction with posterior chamber intraocular lens implantation, (5) any diseases that may cause VF loss or optic disc abnormalities, or (6) inability to perform reliably on automated VF testing. One eye from each participant was scanned and analyzed.

One eye from each participant was selected for analysis. For normal eyes, the eye was randomly selected. For the PPG and PG group, the eye with the worse VF was selected.

• **VISUAL FIELD TESTING:** VF tests were performed with the Humphrey Field Analyzer II (Carl Zeiss, Inc) set for the 24-2 threshold test, size III white stimulus, using the SITA standard algorithm. The macular 6 × 6-mm OCTA scan region corresponds to the central 10° on the VF.[21] Therefore, we used the central VF mean deviation (MD) to calculate the correlations with OCTA parameters. The central 10° VF MD was averaged by the central 16 points in the Humphrey 24-2 VF test. The weight for each VF point is 0.12 for the 4 center points, 0.05 for the 8 edge points, and 0.03 for the 4 corner points.[22]

• **OPTICAL COHERENCE TOMOGRAPHY:** A 70-kHz, 840-nm wavelength spectral-domain OCT system (Avanti RTVue-XR; Optovue Inc) was used.

• **IMAGE ACQUISITION AND PROCESSING:** The macula region was scanned using a 6×6-mm^2 volumetric angiography scan centered on fixation. Each volume was composed of 400 line-scan locations at which 2 consecutive B-scans were obtained. Each B-scan contained 400 A-scans. The AngioVue software used the split-spectrum amplitude-decorrelation angiography algorithm,[23] which compared the consecutive B-scans at the same location to detect flow using motion contrast.[23] Each scan set was composed of 2 volumetric scans: 1 vertical-priority raster and 1 horizontal-priority raster. The AngioVue software used an orthogonal registration algorithm to register the 2 raster volumes to produce a merged 3-dimensional OCT angiogram.[24] Two set of scans were performed within 1 visit.

The merged volumetric angiograms were then exported for custom processing using the Center for Ophthalmic Optics & Lasers–Angiography Reading Toolkit (COOL-ART) software.[25] The OCTA scans contained both volumetric flow (decorrelation) data as well as structural (reflectance) data. Segmentation of the retinal layers was performed by automated MATLAB programs that operate on the structural OCT data. Manual correction of the segmentation was performed when required. We used a reflectance-adjustment method that corrected the artifactually lower flow signal in regions of reduced reflectance (eg, due to pupil vignetting or media opacity). Studies showed that this algorithm was able to remove the dependence of retinal OCTA measurements on the signal strength index and reduce population variation.[5,26] Shadow-removing software was used to reduce artifacts caused by vitreous floaters, pupil vignetting, or defocus present.[27] The projection-resolved algorithm was used to suppress the projection artifact when processing GCLP slabs.[28]

The en face angiograms of ganglion cell layer plexus (GCLP) and superficial vascular complex (SVC) was obtained by maximum flow (decorrelation value) projection. The GCLP has its anterior boundary at the NFL-GCL junction and extends posterior through 75% of the thickness of the combined ganglion cell and inner plexiform layer.[28] SVC is the combination of nerve fiber layer plexus and GCLP. COOL-ART removed flow projection artifacts and calculated reflectance-compensated vessel density (VD)

and capillary density (CD). The VD was defined as the percentage area occupied by the large vessels and microvasculature.

Arterioles and venules (larger vessels) were automatically identified by thresholding the en face mean projection of OCT reflectance within the all-plexus slab. After these larger vessels were excluded, the remaining angiogram was used to compute CD. The VD and CD were evaluated in the 6 × 6-mm scan area excluding 5 pixels (0.075-mm) per edge and the central 1-mm diameter circle, which was manually centered on the fovea based on the en face reflectance image. Four corners (7-mm-diameter circle centered on the fovea) were also excluded because of high coefficient variation in normal eyes.

Using custom software, VD maps were obtained by computing the fraction of area occupied by flow pixels after low-pass filtering 41×41-pixel elements, in SVC and GCLP slab, respectively. Low perfusion was first defined by VD below the 0.5 percentile threshold in the normal reference eyes. Contiguous pixels with low perfusion were grouped to measure the contiguous low-perfusion areas (LPAs). The distribution of contiguous LPAs in normal eyes were examined and its 98.5 percentile cutoff point was 0.12 mm^2. The binary low-perfusion map highlighted abnormally LPAs in red. The LPA in each eye was defined by the cumulative area of pixels that met both low perfusion and contiguity requirements.

The focal perfusion loss (FPL) is the VD loss (relative to the reference map from a healthy population) integrated over the LPA, then expressed as a percentage of the VD integral of the normal reference map. The LPA and FPL were measured from the 6 × 6-mm low-perfusion map, which were global OCTA parameters. To facilitate FPL and VF loss correspondence, LPA and FPL were divided into superior and inferior hemispheric values by a horizontal line crossing the fovea center. We calculated LPA and FPL based on 4 maps: GCLP VD map ($LPA_{GCLP\text{-}VD}$, $FPL_{GCLP\text{-}VD}$), GCLP CD map ($LPA_{GCLP\text{-}CD}$, $FPL_{GCLP\text{-}CD}$), SVC VD map ($LPA_{SVC\text{-}VD}$, $FPL_{SVC\text{-}VD}$), and SVC CD map ($LPA_{SVC\text{-}CD}$, $FPL_{SVC\text{-}CD}$).

The quality of the image was assessed for all OCTA scans. Poor-quality scans with signal strength index below 55 or registered image sets with residual motion artifacts (discontinuous vessel pattern) were excluded from analysis. Two image sets, each meeting the quality criteria, were required to provide data for an assessment of within-visit repeatability. Within-visit repeatability was assessed by the pooled SD and intraclass correlation coefficient.

• **STRUCTURAL OCT ANALYSIS:** Ganglion cell complex (GCC) thickness was measured from the macular scan. The macular GCC thickness was defined as the combination of NFL, GCL, and inner plexiform layer.[29] The GCC focal loss volume (FLV) was output from RTVue software (Optovue Inc). The custom software was used to provide the overall GCC thickness map.

• **STATISTICAL ANALYSIS:** The Student *t* test was used to compare normal and glaucoma groups. Mean ocular perfusion pressure (MOPP) = (⅔ × mean arterial pressure) – intraocular pressure, where mean arterial pressure = (⅔ × diastolic blood pressure) + (⅓ × systolic blood pressure). Pearson correlation was used to determine the relationships between LPA and FPL with the traditional glaucoma measurements of function and structure, such as the VF MD and GCC thickness.

Spearman correlation was also used in the normal group to investigate whether the measurement of LPA and FPL was affected by age, systolic blood pressure, diastolic blood pressure, MOPP, or intraocular pressure. The Cohen κ coefficient is used to measure the localization correspondence between LPA, FPL, and VF. The area under the receiver operating characteristic curve (AROC), sensitivity, and specificity were used to evaluate diagnostic accuracy. The estimated sensitivities for fixed specificities were calculated by MedCalc software using the method of Zhou and associates.[30] All statistical analyses were performed with SPSS 20.0 (SPSS Inc) and MedCalc 10.1.3.0 (MedCalc Software). The statistical significance was assumed at $P < .05$.

RESULTS

• **STUDY POPULATION:** Macular retinal perfusion was studied in 37 healthy participants and 64 with glaucoma. Four participants with glaucoma were excluded because of poor scan quality, leaving 37 healthy participants and 60 with glaucoma for statistical analysis. In the glaucoma group, 30 had PPG, 30 had PG (17 early, 19 moderate, and 4 severe stage according to the Hodapp-Parrish-Anderson classification system[31]). Forty-six glaucoma patients were using at least 1 glaucoma drops. There was no statistically significant difference between the normal and glaucoma groups for intraocular pressure. The glaucoma group was older and had significantly higher MOPP, higher systolic and diastolic blood pressure, and longer axial length (Table 1). Glaucoma participants had significantly worse visual acuity, VF, and structural OCT parameter. The LPA and FPL did not correlate with age, MOPP, systolic blood pressure, diastolic blood pressure, and axial length in the normal group (all $P > .05$) (Table 2).

• **QUALITATIVE ASSESSMENT OF FOCAL CAPILLARY NONPERFUSION:** In normal eyes (Figure 1, first row), the macular GCLP angiogram showed centripetally branching vessels, terminating in the central foveal avascular zone. The VD was higher nasally and gradually decreased temporally. One glaucomatous eye was chosen to demonstrate vessel loss in comparison to the normal eye. It showed VD loss in the inferior hemisphere (Figure 1, second row). In this glaucomatous eye, the arcuate LPA map corresponds to that in both GCLP angiogram and GCLP VD map. The LPA in

TABLE 1. Participant Characteristics

Parameters	Normal (n = 37)	Glaucoma (PPG 30/PG 30) (n = 60)	Difference (*P* Value)
Age, y	59.1±10.4 (41 to 78)	65.8±8.7 (44 to 82)	–6.7 (.001)
Female, n	29 (78.4%)	32 (52.5%)	— (.010)
Glaucoma drops, n	0	1.4	— (<.001)
Visual Acuity, logMAR	0±0.11 (–0.12 to 0.30)	0.06±0.11 (–0.12 to 0.40)	–0.06 (.026)
Intraocular pressure, mm Hg	14.1±2.2 (10 to 19)	14.4±3.2 (9 to 25)	–0.3 (.653)
Diastolic blood pressure, mm Hg	70.5±8.5 (51 to 86)	76.3±12.8 (48 to 120)	–6.2 (.013)
Systolic blood pressure, mm Hg	115.8±12.9 (98 to 156)	125.8±17.6 (80 to 173)	–10.0 (.003)
Mean ocular perfusion pressure, mm Hg	43.0±5.4 (32.7 to 57.0)	47.5±8.4 (26.6 to 64.1)	–4.5 (.003)
Visual field			
MD (dB)	0.3±1.2 (–2.8 to 2.2)	–3.2±4.3 (–16.9 to 2.0)	3.5 (<.001)
PSD (dB)	1.4±0.3 (1.0 to 2.3)	4.5±4.3 (1.1 to 15.2)	–3.1 (<.001)
Structural OCT thickness measurements			
GCC-thickness, μm	101.6±7.6(86.0 to 116.2)	85.3±14.3 (58.2 to 120.3)	16.3 (<.001)
GCC-FLV, %	0.63±0.84 (0 to 3.53)	4.55±4.85 (0 to 16.88)	–3.92 (<.001)
OCTA measurements			
$LPA_{GCLP\text{-}VD}$, mm^2	0.16±0.38 (0 to 1.21)	5.78±6.30 (0 to 21)	–5.61 (<.001)
$FPL_{GCLP\text{-}VD}$, %	0.20±0.47 (0 to 1.71)	7.52±8.84 (0 to 33.42)	–7.31 (<.001)
$LPA_{GCLP\text{-}CD}$, mm^2	0.14±0.30 (0 to 1.19)	6.10±6.74 (0 to 22.05)	–5.96 (<.001)
$FPL_{GCLP\text{-}CD}$, %	0.19±0.42 (0 to 1.70)	9.92±11.70 (0 to 42.10)	–9.73 (<.001)
$LPA_{SVC\text{-}VD}$, mm^2	0.14±0.52 (0 to 2.91)	6.83±7.26 (0 to 23.13)	–6.68 (<.001)
$FPL_{SVC\text{-}VD}$, %	0.14±0.50 (0 to 2.77)	10.06±11.73 (0 to 39.64)	–9.92 (<.001)
$LPA_{SVC\text{-}CD}$, mm^2	0.12±0.42 (0 to 2.39)	6.90±7.47 (0 to 23.99)	–6.78 (<.001)
$FPL_{SVC\text{-}CD}$, %	0.14±0.49 (0 to 2.81)	12.20±14.32 (0 to 49.94)	–12.06 (<.001)

CD = capillary density, dB = decibels, FLV = focal loss volume, FPL = focal perfusion loss, GCC = ganglion cell complex, GCLP = ganglion cell layer plexus, LPA = low perfusion area, MD = mean deviation, PG = perimetric glaucoma, PPG = pre-perimetric glaucoma, PSD = pattern SD, SVC = superficial vascular complex, VD = vessel density.

Data are presented as mean ± SD (range).

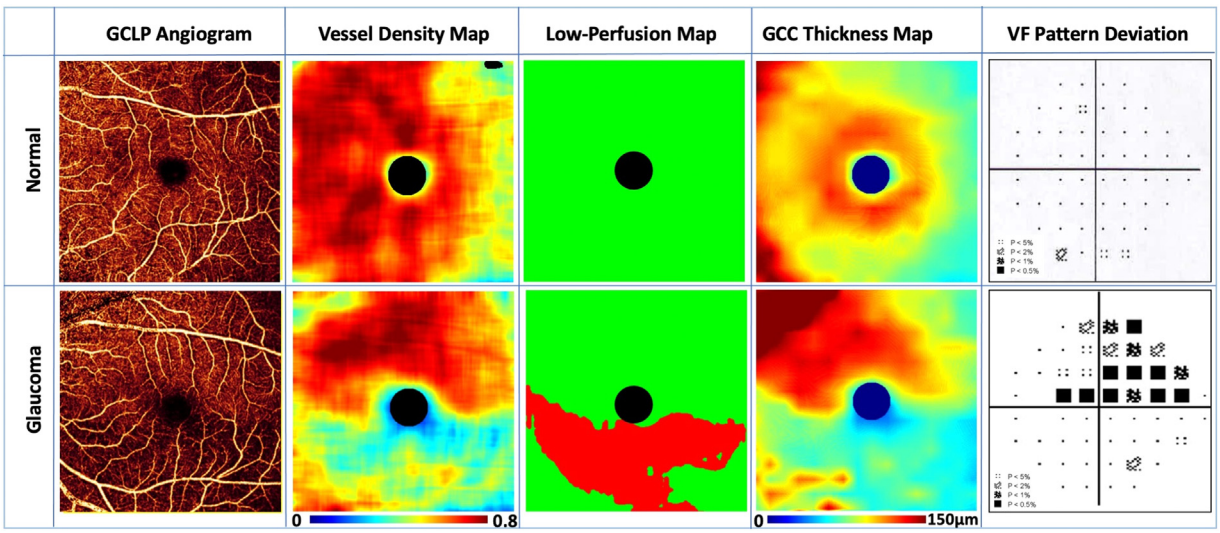

FIGURE 1. A normal and a glaucomatous eye were compared. The glaucomatous eye had lower vessel density in an arcuate pattern in the GCLP angiogram and in the vessel density map, which was highlighted in the low-perfusion map in red. This corresponded to GCC thinning and an inferior visual field defect. (GCC = ganglion cell complex, GCLP = ganglion cell layer plexus.)

TABLE 2. Spearman Correlation of Low Perfusion Area and Focal Perfusion Loss With Clinical Features in the Normal Group.

	LPA-GCLP-VD, *r* (*P* Value)	FPL-GCLP-VD, *r* (*P* Value)
Age	0.148 (.260)	0.140 (.285)
MOPP	0.172 (.188)	0.184 (.159)
SBP	0.147 (.262)	0.160 (.222)
DBP	0.087 (.507)	0.099 (.453)
Axial length	–0.089 (.501)	–0.072 (.584)

DBP = diastolic blood pressure, FPL = focal perfusion loss, GCLP = ganglion cell layer plexus, LPA = low perfusion area, MOPP = mean ocular perfusion pressure, SBP = systolic blood pressure, VD = vessel density.

the inferior region matched well with the VF defects in this glaucomatous eye.

We found $LPA_{GCLP\text{-}VD}$ defects in 29 of 30 eyes in PG, 12 of 30 in PPG, and 4 of 37 in normal eyes. We further analyzed the pattern of perfusion loss using the low perfusion maps (Figure 2). Among the 29 PG eyes with $LPA_{GCLP\text{-}VD}$ defect, 6 eyes had scattered vessel dropout pattern, 8 eyes had arcuate pattern in 1 hemisphere, 12 eyes had a biarcuate pattern in both hemispheres, and 3 eyes had diffused dropout. Among the 12 PPG eyes with $LPA_{GCLP\text{-}VD}$ defect, 10 eyes had scattered vessel dropout pattern, and 2 eyes had arcuate pattern in 1 hemisphere. All 4 normal eyes with $LPA_{GCLP\text{-}VD}$ defects had a scattered pattern.

When analyzing hemispheric $LPA_{GCLP\text{-}VD}$ and $FPL_{GCLP\text{-}VD}$ in the PG eyes, we found significantly more eyes with great inferior than superior defect. For $LPA_{GCLP\text{-}VD}$, 20 eyes had greater inferior than superior, compared to 10 eyes with greater superior than inferior, $LPA_{GCLP\text{-}VD}$ defects ($P = .018$, *t* test). For $FPL_{GCLP\text{-}VD}$, 18 eyes had inferior greater than superior $FPL_{GCLP\text{-}VD}$ ($P = .038$, *t* test).

• GLAUCOMA DIAGNOSTIC ACCURACY AND CORRELATION WITH TRADITIONAL GLAUCOMA DIAGNOSTIC MEASUREMENTS: Both $LPA_{GCLP\text{-}VD}$ and $FPL_{GCLP\text{-}VD}$ were significantly higher in the glaucoma group, compared with normal (Table 1). $LPA_{GCLP\text{-}VD}$ for normal was 0.16 mm^2 in normal, and 5.78 mm^2 for glaucoma (1.49 mm^2 for PPG and 10.07 mm^2 for PG). $FPL_{GCLP\text{-}VD}$ was 0.20% for normal and 7.52% for glaucoma (1.54% for PPG and 13.49% for PG). Both the $LPA_{GCLP\text{-}VD}$ and $FPL_{GCLP\text{-}VD}$ had high diagnostic power for glaucoma (PG+PPG, AROC = 0.85). The diagnostic power was higher with PG (AROC= 0.99) and lower with PPG (AROC = 0.71) (Table 3). Both $LPA_{GCLP\text{-}VD}$ and $FPL_{GCLP\text{-}VD}$ had significantly higher diagnostic power in terms of AROC ($P = .013$ and .016) and sensitivity at 95% specificity than GCC-FLV ($P = .002$ and .013). The diagnostic powers were also higher than global GCLP VD and GCC thickness but the difference was not statistically significant (all $P > .05$).

TABLE 3. The Accuracy of Diagnosing Glaucoma Against the Normal Group by Low Perfusion Area, Focal Perfusion Loss, Global Ganglion Cell Layer Plexus Vessel Density, Ganglion Cell Complex Thickness, and Ganglion Cell Complex Focal Loss Volume

Global Parameters	AROC	95% CI	Sensitivity [a], %
Perimetric glaucoma vs normal			
$LPA_{GCLP\text{-}VD}$	0.993	0.978-1.000	96.7
$FPL_{GCLP\text{-}VD}$	0.990	0.973-1.000	93.3
GCLP VD	0.950	0.889-1.000	83.3
GCC thickness	0.927	0.859-0.994	80.0
GCC FLV	0.957	0.898-1.000	80.0
Preperimetric glaucoma vs normal			
$LPA_{GCLP\text{-}VD}$	0.719	0.591-0.846	36.7
$FPL_{GCLP\text{-}VD}$	0.714	0.586-0.842	30.0
GCLP-VD	0.655	0.527-0.767	30.0
GCC thickness	0.659	0.520-0.799	33.3
GCC FLV	0.531	0.385-0.676	13.3
Glaucoma vs normal			
$LPA_{GCLP\text{-}VD}$	0.855	0.780-0.930	66.7
$FPL_{GCLP\text{-}VD}$	0.851	0.775-0.927	61.7
GCLP VD	0.806	0.718-0.894	56.7
GCC thickness	0.793	0.704-0.882	56.7
GCC FLV	0.824	0.741-0.907	60.0

AROC = area under the receiver operating characteristic curve, FLV = focal loss volume, FPL = focal perfusion loss, GCC = ganglion cell complex, LPA = low perfusion area, SVC = superficial vascular complex, VD = vessel density.
[a]Sensitivity was evaluated at the 95% specificity cutoff.

The $LPA_{GCLP\text{-}VD}$ and $FPL_{GCLP\text{-}VD}$ had good correlation with central 10° VF MD, OCT GCC overall thickness, and GCC-FLV (Table 4; all $P < .001$). Central VF MD correlates significantly better with LPA and FPL compared with its correlation with GCC thickness ($P < .0001$). This showed that perfusion by OCTA parameters correlate better with VF than structural OCT.

• LOCALIZATION OF FPL WITH VF LOSS: We found that $LPA_{GCLP\text{-}VD}$ and $FPL_{GCLP\text{-}VD}$ agreed moderately well regarding the worse hemispheres as identified by central VF. The macular 6 × 6-mm OCTA scan region corresponds to the central 10° VF. We summed up the weighted central 16 points in the Humphrey 24-2 VF test as described in the Method section and defined superior-inferior hemispheric difference in central VF deviation as hemispheric difference outside of the 95% CI found in the normal group (from –1.10 to 1.12 dB). We found 25 PG eyes that had significantly larger deviation difference between superior-inferior hemispheres below –1.10 dB and above 1.12 dB. There was good agreement between central VF MD and $LPA_{GCLP\text{-}VD}$ (Cohen κ 0.655, 95% CI 0.352-0.958, $P < .001$) and between central VF MD and $FPL_{GCLP\text{-}VD}$ (Cohen κ 0.749,

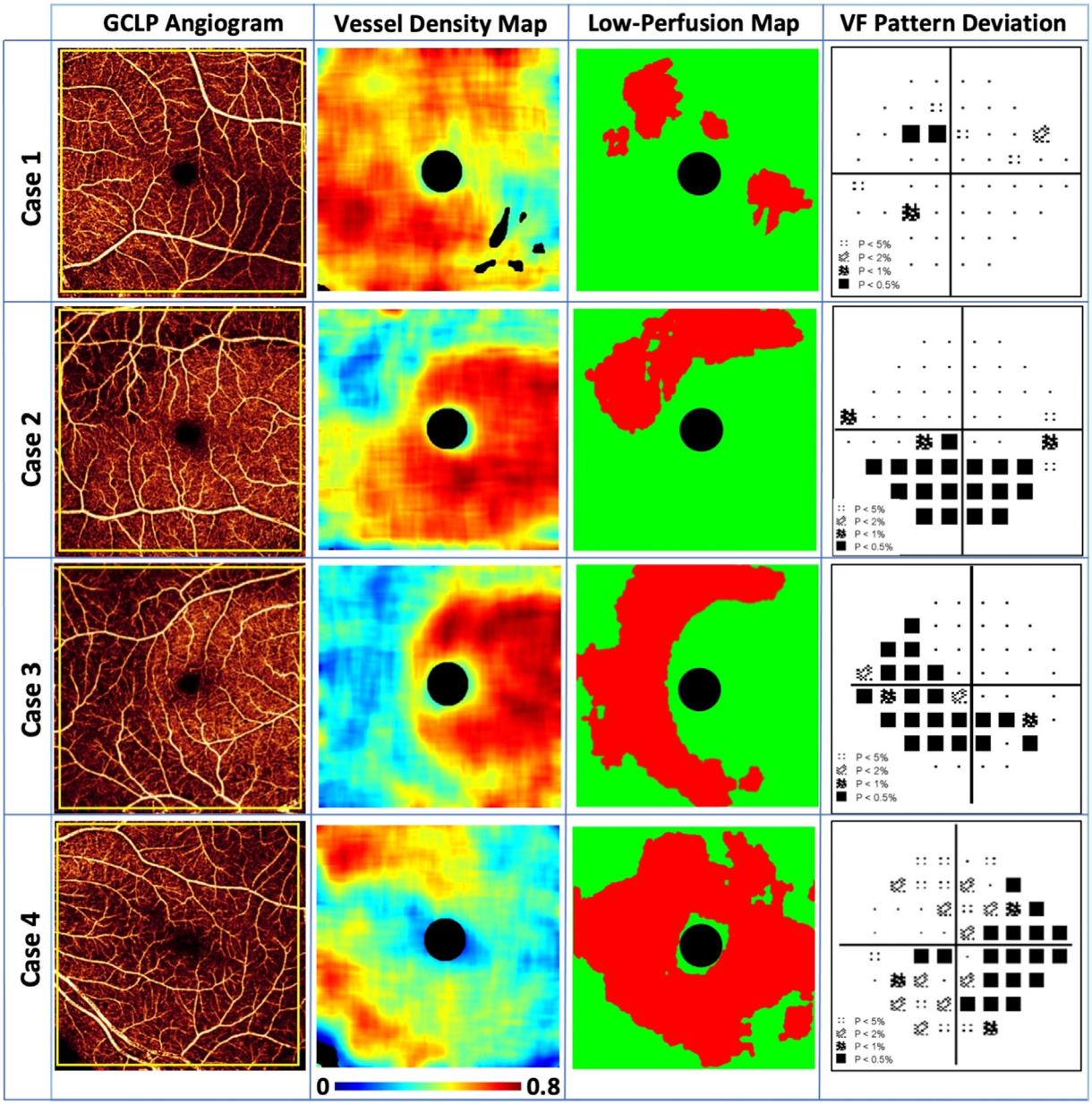

FIGURE 2. In 4 glaucoma cases, Low perfusion map showed 4 microvascular dropout patterns: scatter (case 1), arcuate (case 2), biarcuate (case 3), and diffuse (case 4).

95% CI 0.519-1.000, $P < .001$) in the hemisphere with worse defect. The superior-inferior hemispheric difference for $LPA_{GCLP\text{-}VD}$ and $FPL_{GCLP\text{-}VD}$ also correlated well with the superior-inferior hemifield differences in central VF deviation (Pearson $r = 0.783$ and 0.780, both $P < .001$).

• **REPEATABILITY:** The $LPA_{GCLP\text{-}VD}$ and $FPL_{GCLP\text{-}VD}$ had excellent within-visit repeatability. In the glaucoma group, the intraclass correlation coefficient for $LPA_{GCLP\text{-}VD}$ and $FPL_{GCLP\text{-}VD}$ were 0.956 and 0.951, respectively, and 0.588 and 0.635 in the normal group. The pooled SD of $LPA_{GCLP\text{-}VD}$ and $FPL_{GCLP\text{-}VD}$ were 0.83 mm^2 and 1.82%, respectively. In the normal group, the intraclass correlation coefficient for $LPA_{GCLP\text{-}VD}$ and $FPL_{GCLP\text{-}VD}$ were 0.588 and 0.635, the pooled SD of $LPA_{GCLP\text{-}VD}$ and $FPL_{GCLP\text{-}VD}$ were 0.04 mm^2 and 0.05%, respectively

• **COMPARING LOCAL PERFUSION LOSS CALCULATED BY VESSEL DENSITY AND CAPILLARY DENSITY AND BY GCLP AND SVC SLABS:** We also calculated the LPA and FPL based on the CD map on a GCLP slab ($LPA_{GCLP\text{-}CD}$ and $FPL_{GCLP\text{-}CD}$). The mean values of $LPA_{GCLP\text{-}CD}$ and $FPL_{GCLP\text{-}CD}$ in the glaucoma group were significantly higher (both $P < .01$) than $LPA_{GCLP\text{-}VD}$ and $FPL_{GCLP\text{-}VD}$. However, in terms of glaucoma diagnostic accuracy, the $LPA_{GCLP\text{-}CD}$ and $FPL_{GCLP\text{-}CD}$ did not have statistically

TABLE 4. Pearson Correlation Matrix of Low Perfusion Area, Focal Perfusion Loss, Visual Field, and Structural Variables

Parameters	$FPL_{GCLP\text{-}VD}$	$LPA_{GCLP\text{-}VD}$	Global GCLP VD	GCC Thickness	GCC FLV
$LPA_{GCLP\text{-}VD}$	0.991				
Global GCLP-VD	–0.847	–0.867			
GCC thickness	–0.747	–0.780	0.853		
GCC FLV	0.860	0.834	–0.733	–0.682	
Central VF MD	–0.705	–0.716	0.604	0.566	–0.683
PSD	0.723	0.712	–0.600	–0.538	0.733
VFI	–0.728	–0.729	0.622	0.553	–0.674

FLV = focal loss volume, FPL = focal perfusion loss, GCC = ganglion cell complex, GCLP = ganglion cell layer plexus, LPA = low perfusion area, MD = mean deviation, PSD = pattern SD, VF = visual field, VFI = visual field index.
All $P < .001$.

different AROCs (all $P > .05$) and sensitivities (all $P > .05$) compared with the parameters calculated using VD. Moreover, when we calculated the LPA and FPL with the VD map on an SVC slab ($LPA_{SVC\text{-}VD}$ and $FPL_{SVC\text{-}VD}$), the mean values of $LPA_{SVC\text{-}VD}$ and $FPL_{SVC\text{-}VD}$ in the glaucoma group were statistically higher than the $LPA_{GCLP\text{-}VD}$ and $FPL_{GCLP\text{-}VD}$ (both $P < .001$). However, there were no significant differences between their diagnostic accuracy and correlation with central VF MD when comparing the parameters using SVC slab vs those using GCLP.

DISCUSSIONS

In this study, we apply a novel algorithm to superficial macular retina to create a map of significant perfusion loss. The 2 new OCTA parameters, LPA and FPL, numerically quantify areas of reduced perfusion and severity of the perfusion loss, respectively. The low perfusion map highlights the abnormal contiguous areas of the GCLP in red, whereas LPA sums up the cumulative LPA in millimeters-squared and FPL denotes the severity in percentage. Both macular LPA and FPL are significantly higher in open-angle glaucoma (OAG) compared with controls, signifying a larger and more severe area of macular perfusion loss in OAG. Our finding confirms that OCTA shows decreased microvasculature in macular retina in glaucomatous eyes.

Both macular LPA and FPL have good repeatability and high diagnostic power for OAG. We found that all except 1 patient with perimetric glaucoma had macular perfusion loss using $LPA_{GCLP\text{-}VD}$. The diagnostic ability of LPA and FPL is highest in perimetric glaucoma, with AROC of 0.99 and sensitivity greater than 90% using preset 95% specificity, outperforming overall GCLP-VD and structural OCT GCC thickness. However, in preperimetric glaucoma, LPA and FPL's diagnostic performance decreases significantly, with an AROC of 0.72 and sensitivities of 36.7% (for LPA) and 30.0% (for FPL) at preset 95% specificity, similar to the diagnostic power of OCT GCC thickness.

When all glaucoma (PG+PPG) groups are combined, LPA and FPL have an AROC of 0.85, which is not significantly higher than overall GCLP-VD and OCT overall GCC thickness. Macular LPA and FPL are, therefore, more accurate in diagnosing perimetric than preperimetric primary open angle glaucoma (POAG). One possible explanation is that a 6 × 6-mm macular scan is not sufficient to catch all the early glaucoma vascular damage. The most vulnerable areas of glaucoma damage from the optic nerve include the inferior vulnerability zone, the superior vulnerability zone, and the superonasal wedge, and only a section of the inferior vulnerability zone shows up in the macular scan (termed "macular vulnerability zone").[1] Therefore, if early glaucoma damage occurs outside of this macular vulnerability zone in a PPG eye, it will not be detected in our OCTA macular scan.

When comparing macular LPA and FPL to previously published peripapillary LPA and FPL, we found that the AROC of the macula is lower than that of the peripapillary region published in a previous study.[20] This finding agrees with previous studies that the peripapillary superficial layer may have the highest diagnostic accuracy compared with the macular or optic disc region measured by OCTA.[32] However, in the previous study of peripapillary LPA and FPL, the scan was performed with non-HD OCTA with fewer preperimetric glaucoma patients in the study. Therefore, it is yet to be determined if including more early glaucoma patients with HD scan will change the AROC of peripapillary LPA and FPL.

The advantage of a low-perfusion map in the macula is that it highlights areas of normal perfusion in green and areas of abnormally low perfusion in red. As VD decreased naturally from the nasal to temporal area in the macula, a low-perfusion map helps clinicians to not mistake an area with naturally lower perfusion as an abnormal finding. The red/green color coding also helps clinicians to easily correlate areas of perfusion loss to areas of ganglion cell complex loss in structural OCT. The parameters of LPA summarize the size of the area with abnormally low perfusion. LPA increased from 1.49 mm^2 in preperimetric glaucoma to 10.07 mm^2 in perimetric glaucoma. Similarly, FPA shows that the

severity of perfusion loss increased from 1.54% in preperimetric to 13.49% in perimetric glaucoma.

Macular LPA and FPL correlate moderately well with structural OCT and VF parameters (Table 4). Our finding agrees with other studies that show that macular OCTA VD is associated with GCC thickness measured by structural OCT.[5] The low perfusion map shows a similar pattern of defect in the macula as seen in structural OCT. We also found significantly more inferior greater than superior perfusion loss in glaucomatous eyes, a finding consistent with structural OCT studies that found inferior macular GCC thinning is often deeper and more frequent than superior damage.[1]

With regard to functional correlation, macular LPA and FPL show better correlation to central VF parameter than structural OCT parameters and global OCTA parameters. Many of our findings agree with other studies correlating macular OCTA with central VF parameters. Ghahari and associates[33] found that in advance POAG, OCTA macular VD is more strongly associated with 24-2 VF mean deviation than circumpapillary capillary density or structural OCT thickness. Another study found 3 × 3 mm^2 OCTA macular VD to be associated with a mean sensitivity of 10-2 VF, although the relationship was weaker than the association between GCC thickness and VF MS.[34] In addition, one study found macular vessel density to better correlate with central VF than ganglion cell layer thickness in both advanced and early glaucoma, with superficial vessel density showing the strongest correlation.[35]

In our study, LPA and FPL show stronger correlation than GCC thickness to all 24-2 VF global parameters including MD, pattern SD, and VFI. Despite not having 10-2 VF available, we found a moderately good correlation with central VF deviation and LPA and FPL using a published method to weigh the central points on 24-2. Our finding suggests that using macular LPA and FPL likely will provide better correlation with central VF defect than structural OCT.

The results demonstrate that both SVC and GCLP perform well diagnostically when calculating LPA and FPL, as do CD and VD. Although there is no significant difference in AROC among them, the $LPA_{GCLP\text{-}VD}$ and $FPL_{GCLP\text{-}VD}$ exhibit higher AUC and better repeatability. Therefore, we have selected them as the primary parameters for calculating LPA and FPL.

There are several limitations of the study. This is a cross-sectional study. Therefore, we cannot assess the use of macular LPA and FPL in predicting, and monitoring glaucoma progression. Previous study showing progressive macula VD loss in POAG[16] suggests that our novel parameters could be useful in monitoring glaucoma progression, although a longitudinal study is needed. Second, we did not have 10-2 central VF for more detailed pattern correlation with our 6 × 6-mm macular scan. VF 24-2 test points are spaced 6° apart and has been known to miss small central scotoma seen on 10-2. Therefore, one cannot expect 24-2 to correlated well with the much more detailed GCLP low-perfusion map. VF 10-2 has test points spaced 2° apart, which allows for higher sensitivity to detect smaller scotoma. Therefore, we expect 10-2 to correlate better with GCLP low-perfusion map. Finally, the study has a small sample size, and the findings must be validated in larger studies.

In conclusion, we apply a novel method of mapping and quantifying OCTA perfusion loss to the macular region in glaucoma. Macular LPA and FPL provide an accurate diagnosis of POAG and correlate well with structural GCC thickness and VF severity and location. Nearly all perimetric eyes in our study have significant macular perfusion loss using the new parameters. Further studies are needed to evaluate their use in glaucoma screening and monitoring progression.

CREDIT AUTHORSHIP CONTRIBUTION STATEMENT

Aiyin Chen: Writing – review & editing, Supervision, Resources, Methodology. **Ping Wei:** Writing – original draft, Formal analysis, Data curation. **Jie Wang:** Software, Formal analysis. **Liang Liu:** Data curation. **Acner Camino:** Software. **Yukun Guo:** Software. **Ou Tan:** Methodology. **Yali Jia:** Supervision, Resources. **David Huang:** Writing – review & editing, Supervision.

Funding/Support: The study was supported by NIH grants R01 EY023285, P30 EY010572, and R01 EY010145 from the National Institutes of Health, Oregon Health & Science University (OHSU) foundation, and an unrestricted grant from Research to Prevent Blindness. Financial Disclosures: David Huang and Yali Jia have financial interest in Optovue, Inc, a company that may have a commercial interest in the results of this research and technology. These potential conflicts of interest have been reviewed and are managed by OHSU. The other authors do not report any potential financial conflicts of interest. All authors attest that they meet the current ICMJE criteria for authorship.

REFERENCES

1. Hood DC. Improving our understanding, and detection, of glaucomatous damage: An approach based upon optical coherence tomography (OCT). *Prog Retin Eye Res*. 2017;57:46–75.
2. Hood DC, Slobodnick A, Raza AS, de Moraes CG, Teng CC, Ritch R. Early glaucoma involves both deep local, and shallow widespread, retinal nerve fiber damage of the macular region. *Invest Ophthalmol Vis Sci*. 2014;55:632–649.
3. Curcio CA, Allen KA. Topography of ganglion cells in human retina. *J Comp Neurol*. 1990;300:5–25.
4. Iwasaki M, Inomata H. Relation between superficial capillar-

ies and foveal structures in the human retina. *Invest Ophthalmol Vis Sci*. 1986;27:1698–1705.
5. Takusagawa HL, Liu L, Ma KN, et al. Projection-resolved optical coherence tomography angiography of macular retinal circulation in glaucoma. *Ophthalmology*. 2017;124:1589–1599.
6. Akil H, Chopra V, Al-Sheikh M, et al. Swept-source OCT angiography imaging of the macular capillary network in glaucoma. *Br J Ophthalmol*. 2017 Published online August 9. doi:10.1136/bjophthalmol-2016-309816.
7. Jeon SJ, Park HL, Park CK. Effect of macular vascular density on central visual function and macular structure in glaucoma patients. *Sci Rep*. 2018;8:16009.
8. Richter GM, Madi I, Chu Z, et al. Structural and functional associations of macular microcirculation in the ganglion cell-inner plexiform layer in glaucoma using optical coherence tomography angiography. *J Glaucoma*. 2018;27:281–290.
9. Huang JY, Pekmezci M, Mesiwala N, Kao A, Lin S. Diagnostic power of optic disc morphology, peripapillary retinal nerve fiber layer thickness, and macular inner retinal layer thickness in glaucoma diagnosis with fourier-domain optical coherence tomography. *J Glaucoma*. 2011;20:87–94.
10. Liu L, Jia Y, Takusagawa HL, et al. Optical coherence tomography angiography of the peripapillary retina in glaucoma. *JAMA Ophthalmol*. 2015;133:1045–1052.
11. Liu L, Edmunds B, Takusagawa H, et al. Projection-resolved optical coherence tomography angiography of the peripapillary retina in glaucoma. *Am J Ophthalmol*. 2019;207:99–109.
12. Takusagawa HL, Liu L, Ma KN, et al. Projection-resolved optical coherence tomography angiography of macular retinal circulation in glaucoma. *Ophthalmology*. 2017;124(11):1589–1599.
13. Yarmohammadi A, Zangwill LM, Manalastas PIC, et al. Peripapillary and macular vessel density in patients with primary open-angle glaucoma and unilateral visual field loss. *Ophthalmology*. 2018;125:578–587.
14. Yarmohammadi A, Zangwill LM, Diniz-Filho A, et al. Optical coherence tomography angiography vessel density in healthy, glaucoma suspect, and glaucoma eyes. *Invest Ophthalmol Vis Sci*. 2016;57:OCT451–OCT459.
15. Jia Y, Wei E, Wang X, et al. Optical coherence tomography angiography of optic disc perfusion in glaucoma. *Ophthalmology*. 2014;121:1322–1332.
16. Shoji T, Zangwill LM, Akagi T, et al. Progressive macula vessel density loss in primary open-angle glaucoma: a longitudinal study. *Am J Ophthalmol*. 2017;182:107–117.
17. Asrani S, Edghill B, Gupta Y, Meerhoff G. Optical coherence tomography errors in glaucoma. *J Glaucoma*. 2010;19:237–242.
18. Ray R, Stinnett SS, Jaffe GJ. Evaluation of image artifact produced by optical coherence tomography of retinal pathology. *Am J Ophthalmol*. 2005;139:18–29.
19. Hoh ST, Lim MC, Seah SK, et al. Peripapillary retinal nerve fiber layer thickness variations with myopia. *Ophthalmology*. 2006;113:773–777.
20. Chen A, Liu L, Wang J, et al. Measuring glaucomatous focal perfusion loss in the peripapillary retina using OCT angiography. *Ophthalmology*. 2020;127:484–491.
21. Hood DC, Raza AS. On improving the use of OCT imaging for detecting glaucomatous damage. *Br J Ophthalmol*. 2014;98(Suppl 2) ii1-9.
22. Hood DC, Raza AS. Method for comparing visual field defects to local RNFL and RGC damage seen on frequency domain OCT in patients with glaucoma. *Biomed Opt Express*. 2011;2:1097–1105.
23. Jia Y, Bailey ST, Hwang TS, et al. Quantitative optical coherence tomography angiography of vascular abnormalities in the living human eye. *Proc Natl Acad Sci U S A*. 2015;112:E2395–E2402.
24. Kraus MF. Motion correction in optical coherence tomography volumes on a per A-scan basis using orthogonal scan patterns. *Biomed Opt Express*. 2012;3(6):1182–1199.
25. Zhang M, Wang J, Pechauer AD, et al. Advanced image processing for optical coherence tomographic angiography of macular diseases. *Biomed Opt Express*. 2015;6:4661–4675.
26. Gao SS, Jia Y, Liu L, et al. Compensation for Reflectance Variation in Vessel Density Quantification by Optical Coherence Tomography Angiography. *Invest Ophthalmol Vis Sci*. 2016;57:4485–4492.
27. Camino A, Jia Y, Yu J, Wang J, Liu L, Huang D. Automated detection of shadow artifacts in optical coherence tomography angiography. *Biomed Opt Express*. 2019;10:1514–1531.
28. Hagag AM, Wang J, Lu K, et al. Projection-resolved optical coherence tomographic angiography of retinal plexuses in retinitis pigmentosa. *Am J Ophthalmol*. 2019;204:70–79.
29. Tan O, Chopra V, Lu AT, et al. Detection of macular ganglion cell loss in glaucoma by Fourier-domain optical coherence tomography. *Ophthalmology*. 2009;116 2305-14e1-2.
30. Zhou X-H, McClish Donna K, Obuchowski Nancy A. *Statistical Methods in Diagnostic Medicine*. John Wiley & Sons; 2009.
31. Hodapp E, Parrish R, Anderson D. *Clinical Decisions in Glaucoma*. Mosby-Year Book, Inc; 1993.
32. Bekkers A, Borren N, Ederveen V, et al. Microvascular damage assessed by optical coherence tomography angiography for glaucoma diagnosis: a systematic review of the most discriminative regions. *Acta Ophthalmol*. 2020;98(6):537–558.
33. Ghahari E, Bowd C, Zangwill LM, et al. Association of macular and circumpapillary microvasculature with visual field sensitivity in advanced glaucoma. *Am J Ophthalmol*. 2019;204:51–61.
34. Penteado RC, Zangwill LM, Daga FB, et al. Optical coherence tomography angiography macular vascular density measurements and the central 10-2 visual field in glaucoma. *J Glaucoma*. 2018;27:481–489.
35. Hwang HS, Lee EJ, Kim H, Kim TW. Relationships of macular functional impairment with structural and vascular changes according to glaucoma severity. *Invest Ophthalmol Vis Sci*. 2023;64:5.